Analysis of the Structure and Stability of a Backbone-Modified Oligonucleotide: Implications for Avoiding Product Inhibition in Catalytic Template-Directed Synthesis

Peizhi Luo, John C. Leitzel, Zheng-Yun J. Zhan, and David G. Lynn*

Contribution from the Searle Chemistry Laboratory, 5735 Ellis Avenue, Department of Chemistry, The University of Chicago, Chicago, Illinois 60637

Received August 14, 1997

Abstract: The structural and thermodynamic origins of the destabilization of a backbone-modified DNA duplex **1**, formed between d(CpGpT$_N$TpGpC), containing a single aminoethyl group (−CH_2−CH_2−NH_2^+−) in place of the phosphodiester (−O−PO_2^-−O−) linkage of the central TT dimer, and d(GpCpApApCpG) are investigated. Analyses for the corresponding native duplex and two other related structural analogues of duplex **1** have been compared. Duplex **1** shows a cooperative thermal melting transition that is consistent with a two-state process. At a 2 mM concentration, the melting temperature of duplex **1** is reduced by 17 °C from the native duplex, and this decrease in stability is further assigned to an unfavorable decrease in enthalpy of 7 kcal mol^{-1} and a favorable increase in entropy of 15 eu mol^{-1}. NMR structural analysis shows that the modified duplex **1** still adopts a canonical B-DNA conformation with Watson−Crick base pairing preserved; however, the CH_2 group that replaces the native PO_2^- group in the modified backbone is flexible and free to collapse onto a hydrophobic core formed by the base edges and sugar rings of the flanking TT/AA nucleosides of the duplex. This conformation is significantly different from the maximally solvent-exposed orientation of the native phosphate in DNA. The entropic origin of the 15 eu mol^{-1} difference between the native and the modified duplex **1** is attributed to the hydrophobic interaction between the collapsed ethylamine linkage with the hydrophobic core of duplex **1**. This assignment is further supported by a favorable comparison between the observed change in entropy and the estimated value for the hydrophobic interaction around the modified region. This estimated value is based on recent experimental measurement of the hydrophobic interaction between aliphatic groups and nucleic acids as well as ethylamine solvent transfer data. The overall decrease in the stability of duplex **1** results from a decrease in base stacking and hydrogen-bonding interactions between the base pairs. A model is, therefore, proposed to explain how the change in the local backbone conformation could disrupt the long-range cooperativity of DNA duplex formation upon backbone modifications. These studies provide an approach for identifying the factors that control the stability of the nucleic acid duplex structures containing backbone modifications, with direct implication for designing antisense oligonucleotides and template-directed reactions containing non-native phosphodiester linkages.

Introduction

Zamecnik and Stephenson[1] first showed that synthetic oligonucleotides could be used to block gene expression by binding specifically with complementary sequences of target mRNAs. Over the past decade the efforts to modify native phosphodiester linkages to improve nuclease resistance and membrane permeation of naturally occurring oligonucleotides for therapeutic applications have been extensive.[2] These neutral backbone-modified oligonucleotides generally show attenuated binding affinity to their complementary RNA strand relative to the corresponding nucleic acid.[2e,f,3] These studies have therefore clearly demonstrated that it is possible to tune nucleic acid duplex stability with structural variation of the backbone linkage. Product inhibition severely limits template-directed reactions,[4] and this insight into the control of duplex stability has recently made it possible to design reactions that catalytically translate the information encoded in DNA into different polymer backbones.[5]

This catalytic reaction involves the template-directed reductive ligation of an imine to a product, d(CpGpT$_N$TpGpC), containing a single aminoethyl group (−CH_2−CH_2−NH_2^+−) replacing the normal TT phosphodiester linkage. The catalytic cycle exploited the observation that the duplex formed between the backbone-modified product and its complementary d(GpCpApApCpG) template, **1**, is substantially destabilized relative to the substrate

* Voice mail and fax: (312) 702-7063. E-mail: d-lynn@uchicago.edu.

(1) (a) Zamecnik, P. C.; Stephenson, M. L. *Proc. Natl. Acad. Sci. U.S.A.* **1978**, 75, 280. (b) Stephenson, M. L.; Zamecnik, P. C. *Proc. Natl. Acad. Sci. U.S.A.* **1978**, 75, 285.

(2) (a) De Mesmaeker, A.; Waldner, A.; Lebreton, J.; Hoffmann, P.; Fritsch, V.; Wolf, R.; Miller, P. S. In *Oligonucleotides: Antisense Inhibitors of Gene Expression*; Cohen, J. S., ed.; CRC Press: Boca Raton, FL, 1989, pp 79−93. (b)Uhlmann, E.; Peyman, A. *Chem. Rev.* **1990**,*90*, 544. (c) Carruthers, M. H. *Acc. Chem. Res.* **1991**, *24*, 278. (d) Varma, R. S. *Synlett* **1993**, 621. (e) De Mesmaeker, A.; Altmann, K.-H.; Waldner, A.; Wendeborn, S. *Curr. Opin. Struct. Biol.* **1995**, *5*, 343. (f) De Mesmaeker, A.; Häner, R.; Martin, P.; Moser, H. E. *Acc. Chem. Res.* **1995**, *28*, 366.

(3) Egli, M. *Angew. Chem., Int. Ed. Engl.* **1996**, *35*, 1894.

(4) (a) Naylor, R.; Gilham, P. T. *Biochemistry* **1966**, *5*, 2722. (b) Orgel, L. E. *Nature* **1992**, *358*, 203. (c) Hong, J.-I.; Feng, Q.; Rotello, V.; Rebek, J. *Science* **1992**, *255*, 848. (d) Li, T.; Nicolaou, K. C. *Nature* **1994**, *369*, 218. (e) Ertem, G.; Ferris, J. P. *Nature* **1996**, *379*, 238. (f) Sievers, D.; von Kiedrowski, G. *Nature* **1994**, *369*, 221.

(5) (a) Goodwin, J. T.; Lynn, D. G. *J. Am. Chem. Soc.* **1992**, *114*, 9197. (b) Goodwin, J. T.; Luo, P. Z.; Leitzel, J. C.; Lynn, D. G. In*Self-Production of Supramolecular Structures: From Synthetic Structures to Models of Minimal Living Systems*, Fleischaker, G. R., Colonna, S., Luisi, P. L., Eds.; Kluwer Academic Publishers: Dordrecht, The Netherlands, 1994; pp 99−104. (c) Zhan, Z.-Y. J.; Lynn, D. G. *J. Am. Chem. Chem. Soc.* **1997**, *119*, 12420−12421.

S0002-7863(97)02869-2 CCC: $15.00
Published on Web 03/21/1998

Scheme 1. Synthesis of the Modified DNA Dimers[a]

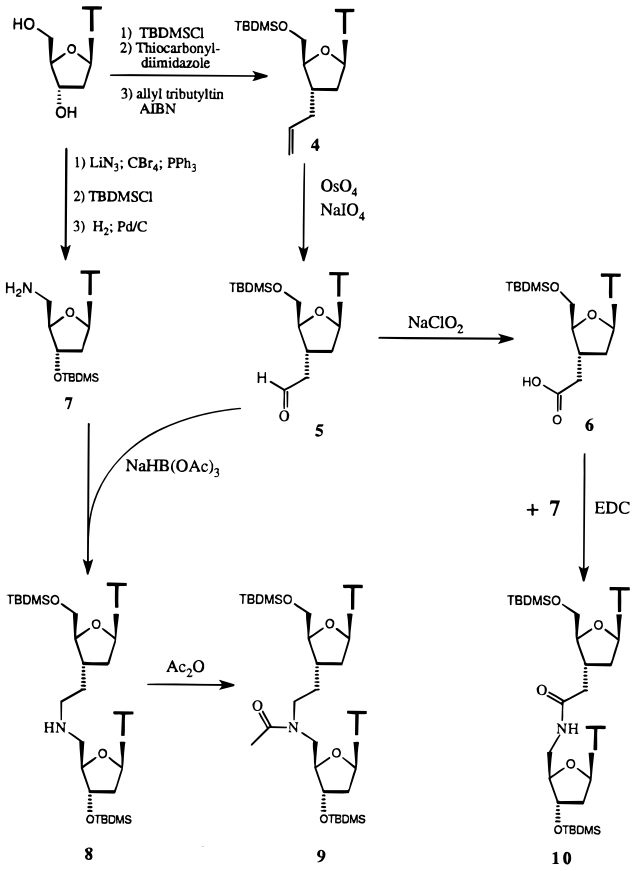

[a] Dimers shown were subsequently converted to phosphoramidates and incorporated into DNA oligomers.

imine. The difference in the thermal melting temperature was as high as 15 °C,[5c] but the structural and energetic origins of the altered stability have not been defined.[2−5]

In contrast with the explosive growth in synthesizing backbone-modified oligonucleotides, only limited progress has been made in determining the structural and energetic factors which control the stability of the duplexes.[3] De Mesmaeker et al.[2e,f] have reviewed the chemical modifications and the stability of the second generation antisense oligonucleotides that contain no phosphorus atom in the modified linkages. The hybridization stability of these duplexes, as measured by the thermal melting temperature, is rationalized in terms of the change in charge, conformational rigidity, structural preorganization, hydrophobicity, and steric hindrance differences (see Figures 5 and 6 and Table 1 in ref 2f). In principle, structural studies by NMR and X-ray can provide important insight into the origins of the changes in enthalpy and entropy resulting from backbone modifications. However, the thermodynamic analyses depend heavily on the thermal melting temperature,[2d−f] which involves a complex interplay between the enthalpic and entropic components of the duplexes and/or the single strands.[3] We saw the following issues relating to the structure and stability of the backbone-modified oligonucleotides as critical to any such analysis: (1) Since the formation of a nucleic acid duplex is highly cooperative, could a chemical modification in the middle of one strand change the coopertivity of duplex formation, deviating, for example, from the usual two-state thermal transition? (2) Can the thermodynamic stability be dissected into changes in enthalpy and entropy of the modified duplex relative to its native analogue? (3) Is the difference between the stability of the modified duplex and the native duplex caused by a change in the duplex structure, the modified single strand, or both? Although the comparisons between a backbone-modified duplex with its native analogue have generally assumed that only the duplex stability, rather than the single strand, has been changed upon backbone modification, the experimental basis for such an implicit assumption is not yet clear. (4) What is the overall structure in the modified duplex as compared to its native analogue? Is it still nativelike, retaining the general features characteristic of the native duplex, or is the structure significantly altered? If the overall structure of the native duplex is preserved upon backbone modification, is it possible to detect structural changes around the modified region? (5) Finally, can any global and local structural changes be related to changes in ΔS and ΔH values?

As a specific example to illustrate the points listed above, we have studied the short DNA duplex, **1**, formed between d(CpGpT$_N$TpGpC) and its complementary d(GpCpApApCpG) strand. A single phosphodiester is replaced by the aminoethyl group,[5] and the approach taken is similar in spirit to studies of point mutations on protein stability. A comparison is made of the melting curves obtained for duplex **1**, and its analogues, with the native DNA sequence. Both UV and NMR analyses, under differing salt and sample concentration conditions, are employed, and the thermal unfolding curves are dissected into changes in enthalpy and entropy. For the native DNA duplex, quantitative comparisons are made among values derived from UV and NMR measurements as well as from calculated values from the literature. NMR measurements show that the structure of duplex **1** is nativelike and maintains the Watson−Crick base pairs as exhibited by similar cross-peak patterns characteristic of the native duplex. However, significant perturbation in the modified TT region is detected using the NOE cross-peaks between the two methylenes of the aminoethyl linkage and the flanking sugar protons. This result allows for a rationalization of the changes in enthalpy and entropy of the backbone-modified duplex to the observed local and global structural changes. These results have allowed a model to be proposed which attempts to explain the observed destabilization of backbone-modified oligonucleotides with neutral linkers. One important implication underlying this model, as well as others proposed recently,[6] is the role that the polyanionic phosphate backbone plays in conferring duplex stability. The comprehensive approach that we have taken should be useful for analyzing other backbone-modified nucleic acids and allow the factors that control duplex stability to be better defined.

Results

Synthesis of Modified Nucleosides. The hexameric template, d(GpCpApApCpG), was designed to be small, palindromic, and non-self-complementary, and to have a high G/C content to enhance association.[3] The central template adenosine residues simplified the synthetic chemistry to modifications of thymidine (Scheme 1). The ease of radical allylation at C-3′ (60% recrystallized yield over three steps) set the stereochemical position of the aldehyde that was ultimately generated by oxidative cleavage.[3a] Only the generation of the 5′-amine was required on the second thymidine derivative. For bulk systhesis, reductive amination of the 3′-carboxyaldehyde **5** with the 5′-amine **7** gave the amine-linked dimer **8** in >95% purified yield.[3a,7] Acetylation of **8** gave cleanly the *N*-acyl dimer **9**, and further oxidation of **5** to **6** and condensation with **7** gave the amide dimer **10**. Each of these dimers was converted into the

(6) Richert, C.; Roughton, A. L.; Benner, S. A. *J. Am. Chem. Soc.* **1996**, *118*. 4518.

Scheme 2. Modified DNA Duplex with the TT Dimer Region As Indicated[a]

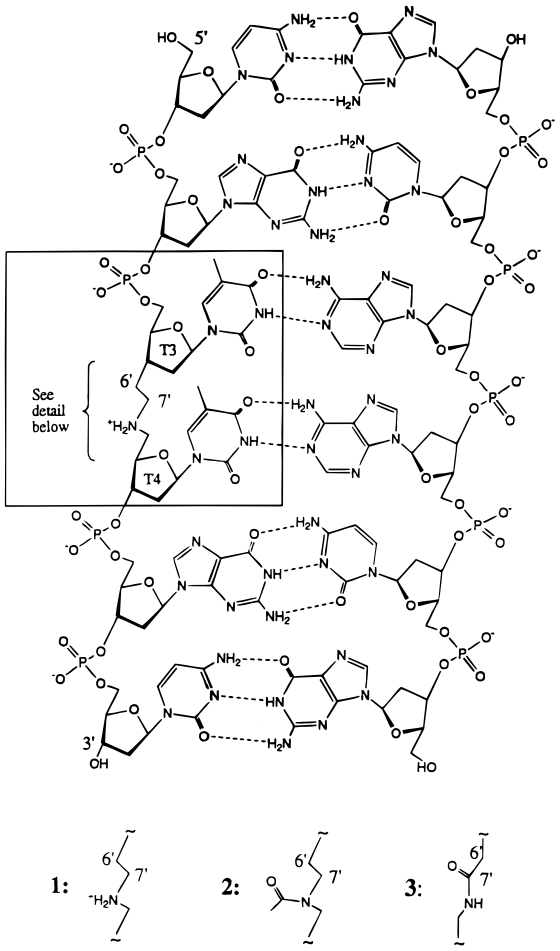

1: **2:** **3:**

[a] Three linkages in the TT dimer are shown: **1**, aminoethyl; **2**, *N*-acetylaminoethyl; **3**, amide.

appropriate phosphoramidite for incorporation into the hexanucleotide via solid-phase synthesis. This approach permitted the ready synthesis of **1** as well as the modified hexamers **2** and **3** shown in Scheme 2.

Thermodynamic Measurements. Strand association was analyzed with both UV and NMR spectroscopies, and different methods for extracting the thermodynamic values were explored. In all cases, attempts were made to fit the data to a simple equilibrium between the DNA duplex and the single strands. In this two-state model, the equilibrium constant, *K*, for association of non-self-complementary strands is expressed by eq 1, where C_T is the total concentration of oligonucleotide strands and *f* is the fraction of strands in the duplex form.[8a,b]

$$K = 2f/[(1 - f)^2 C_T] \quad (1)$$

UV Analyses. The melting temperature, T_m, of the native duplex was determined via the hypochromic shift of the base transition at five different concentrations in 500 mM NaCl. The ΔH and ΔS values were derived from the slope and intercept, respectively, of a plot of $\ln(C_T/4)$ vs $1/T_m$ in Figure 1, according

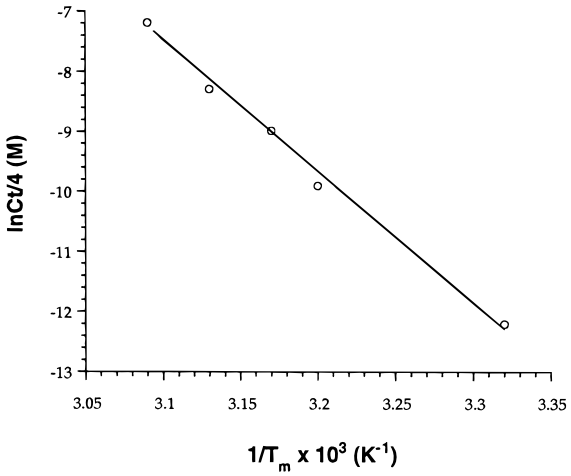

Figure 1. $\ln(C_T/4)$ vs $1/T_m$ for the native duplex in 500 mM NaCl, 10 mM NaH_2PO_4, 2 mM NaN_3, pH 6 buffer.

to eq 2a,[8a,b] or alternatively from a nonlinear least-squares fit to eq 2b, where C_d is the duplex concentration. The nonlinear

$$\ln(C_T/4) = (\Delta H/R)(1/T_m) - (\Delta S/R) \quad (2a)$$

$$C_d = 2\exp((\Delta H/R)(1/T_m) - (\Delta S/R)) \quad (2b)$$

least-squares analysis has the advantage of fitting the thermodynamic functions and baseline parameters simultaneously to the primary data. This approach avoids the empirical assumption of the linear baseline regions at the low- and high-temperature limits. Both approaches gave identical values of ΔH and ΔS (Table 1); however, as expected, the errors are much larger with the least-squares fit. At a 67% confidence level, the error was 7 times larger. A similar increase in error was previously noted by Santoro and Bolen[9] in determinations of the ΔG of protein unfolding.

NMR Analyses. The design of the template placed two adenine bases in the center of the duplex. The two aromatic methyls of the thymidine bases in the complementary strand, T3-CH_3 and T4-CH_3, reside in the center of the duplex and flank the site of the structural change that is under consideration. The chemical shifts of these methyl protons in the native and the modified duplex **1** show cooperative thermal transitions with temperature only when measured in the presence of the template strand (Figure 2a). In addition to being able to monitor the center of the duplex, these NMR analyses have several other advantages. First, the higher concentrations of the nucleic acids used in the NMR experiments move the T_m for these short strands above room temperature in H_2O. Second, the baselines for the duplex, δ_d, and the single strands, δ_s, are well defined (Figure 2a). Finally, the exchange rate between the two states is fast on the NMR time scale. When the observed chemical shift, δ_{obs}, is modeled as a function of these two states, eq 3,[10] the resulting van't Hoff plots from eq 4, Figure 2b, give ΔH

$$\delta_{obs} = (1 - f)\delta_s + f\delta_d \quad (3)$$

$$\ln K = -(\Delta H/R)(1/T) + (\Delta S/R) \quad (4)$$

and ΔS values for both the T3-CH_3 and T4-CH_3 groups that

(7) Caulfield, T. J.; Prasad, C. V. C.; Prouty, C. P.; Saha, A. K.; Sardaro, M. P.; Schairer, W. C.; Yawman, A.; Upson, D. A., & Kruse, L. I. *Bioorg. Med. Chem. Lett.* **1993**, *3*, 2771.

(8) (a) Borer, P. N.; Dengler, B.; Tinoco Jr, I.; Uhlenbeck, O. C. *J. Mol. Biol.* **1974**, *86*, 843. (b) Albergo, D. D., Marky, L. A., Breslauer, K. J.; Turner, D. H. *Biochemistry* **1981**, *20*, 1409. (c) Albergo, D. D.; Turner, D. H. *Biochemistry* **1981**, *20*, 1413.

(9) Santoro, M. M.; Bolen, D. W. *Biochemistry* **1988**, *27*, 8063.

(10) (a) Tran-Dinh, S.; Neumann, J.-M.; Huynh-Dinh, T.; Genissel, B.; Igolen, J.; Simonnot, G. *Eur. J. Biochem.* **1982**, *124*, 415. (b) Pieter, J.; Mellema, J.-R.; Van Den Elst, H.; Van Der Marel, G.; Van Boom, J.; Altona, C. *Biopolymers* **1989**, *28*, 741.

Table 1. Thermodynamic Parameters of Thermal Unfolding from the Native Duplex and the Backbone-Modified Duplex **1** to Coiled Strands[a]

thermodynamic parameters	predicted[b] (native)	UV melt[c] (native)	T3CH$_3$[d] (native)	T3CH$_3$[d] (duplex **1**)	T4CH$_3$[d] (native)	T4CH$_3$[d] (duplex **1**)
$-\Delta$H (kcal mol^{-1})	44.4	43.6 ($\pm$1.8)	47.3 ($\pm$1.3)	40.2 ($\pm$0.9)	46.1 ($\pm$2.5)	39.1 ($\pm$1.7)
difference in $-\Delta H$ between native and modified duplex **1**				7.1		7.0
$-\Delta S$ (eu mol^{-1})	126.1	120.2 ($\pm$5.8)	136.9 ($\pm$4.0)	121.4 ($\pm$3.0)	131.9 ($\pm$8.2)	117.1 ($\pm$5.7)
difference in $-\Delta S$ between native and modified duplex **1**				15.5		14.8

[a] The results are derived from the van't Hoff plots in Figures 1b and 2b. [b] Predicted values were calculated using the nearest-neighbor thermodynamic data[11a] at 1 M NaCl, pH 7. The 126.1 eu mol^{-1} was derived from the predicted ΔH and ΔG using the nearest-neighbor approximation. [c] UV melting at different DNA concentrations in 500 mM NaCl, 10 mM NaH_2PO_4, 2 mM NaN_3, pH 6. [d] The change in chemical shift with temperature as monitored by T3 and T4 methyl groups at 2 mM total oligonucleotide concentration in 100 mM NaCl, 10 mM NaH_2PO_4, 2 mM NaN_3, pH 6.

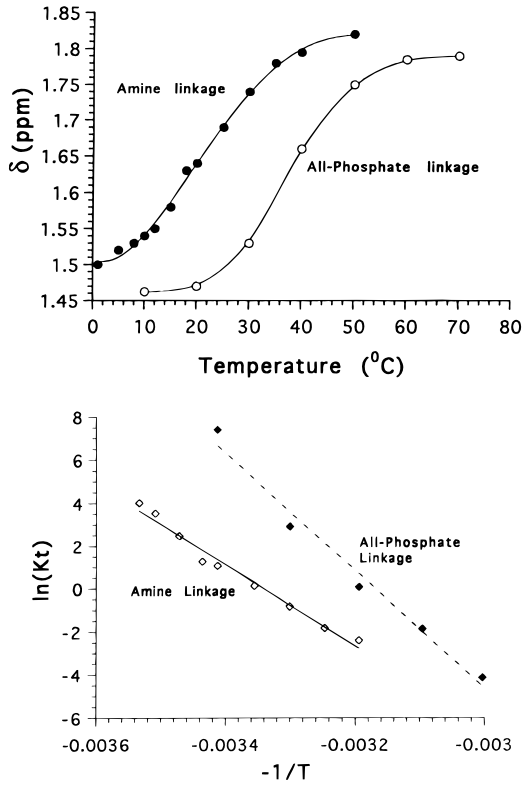

Figure 2. (a, top) Chemical shift change of the T3 methyl groups in the native (●) and the modified duplex **1** (○) as a function of temperature. The curves through data points are fitted to eq 5 using the nonlinear least-squares method. Lines through each melting profile are fit with either floating or fixed baseline parameters in δ_s and δ_d. The difference in T_m between native and modified duplex **1** is ca. 17 °C in 2 mM solutions in 9:1 (v/v) H_2O-D_2O, 100 mM NaCl, 10 mM NaH_2PO_4, 2 mM NaN_3, pH 6 buffer. (b, bottom) van't Hoff plots of the thermal unfolding profiles for the native (◆) and modified duplex **1** (◇).

are in close agreement with those determined from UV analysis (Table 1). By combining eqs 1 and 3, the change in chemical shift can be fit to eq 5, where T is the temperature in Kelvin, R

$$\delta_{obs} = \delta_s + (\delta_d - \delta_s)(1 + c - ((1 + c)^2 - 1)^{1/2})$$

$$c = 1/(C_T K) = (1/C_T)\exp(\Delta H/(RT) - \Delta S/R) \qquad (5)$$

is the gas constant, and δ_s, δ_d, ΔH, and ΔS are the parameters in the nonlinear least-squares analysis. By this method, the T3-CH$_3$ gives $\Delta H = -45.5$ kcal mol^{-1} and $\Delta S = -131$ eu mol^{-1}, in general agreement with the direct van't Hoff analysis, but again the error is 8−9 times greater. Holding the baseline parameters of δ_d and δ_s at the values used in the van't Hoff analysis, this error is reduced 3-fold, consistent with the floating baselines being largely responsible for the errors.[9]

Justifying the Analyses. The calculated ΔH value for this sequence, using the nearest-neighbor approximation of Breslauer et al.,[11a] is -44.4 kcal mol^{-1}. These estimated ΔH values for short oligonucleotide duplexes give excellent agreement with calorimetry measurements.[8a,b,11a] The ratio of the UV-determined ΔH to this calculated value is 0.98, justifying the use of the two-state assumption for duplex melting.[8b]

Although UV analyses have been used extensively for measuring the global unfolding of DNA duplexes, the $\Delta\delta$ of the thymidine methyl resonances may be diagnostic of a more localized perturbation. These methyls, which reside in the center of the duplex, yield ΔH values that are of the same order, -47.3 kcal mol^{-1} from T3-CH$_3$ and -46.1 kcal mol^{-1} from T4-CH$_3$, but slightly more negative than those from calculations (Table 1). The more negative values may result from the cooperative transition monitored only at the center of the duplex, free from the fraying of base pairs at the ends, or from the isotope effect in D_2O.[8b]

The ΔS value was also calculated from the predicted ΔG and ΔH of Breslauer et al.[11a] to be -126 eu mol^{-1} in 1 M NaCl. By UV in 500 mM NaCl, $\Delta S = -120 \pm 5.8$ eu mol^{-1}; by NMR in 100 mM NaCl, $\Delta S = -137 \pm 4.0$ and -132 ± 8.2 eu mol^{-1} from T3-CH$_3$ and T4-CH$_3$, respectively. These differences in ΔS are accounted for quantitatively by the difference in salt concentrations used in the experiments. According to the polyelectrolyte theory of nucleic acids,[12] the salt effect is primarily of entropic origin that arises from counterion condensation on the phosphate backbones of the duplex, and this assignment is supported by precise scanning microcalorimetry measurements.[13] By substituting the concentration of NaCl into eq 6, where C is the molar salt concentration and R is the gas constant, the change in entropy due to the salt effect on duplex

$$\Delta S = (-1.11 + 0.36 \log C)R \quad \text{eu mol}^{-1} \text{ of phosphate} \qquad (6)$$

melting is predicted as 2.9, 2.4, and 2.2 eu mol^{-1} of phosphate at 100 mM, 500 mM, and 1 M NaCl, respectively. If the NaCl concentration is changed from 100 mM to 1 M, the increase in ΔS upon duplex formation is predicted to be 0.7 eu mol^{-1} of phosphate or 7 eu mol^{-1} of a hexamer duplex containing 10 phosphate groups. The predicted increase of 7 eu mol^{-1} in ΔS upon duplex formation going from 100 mM to 1 M NaCl lies within the observed difference range of 11 eu mol^{-1} from T3-CH$_3$ and 5.8 eu mol^{-1} from T4-CH$_3$ by NMR and the calculated ΔS at 1 M NaCl (Table 1). The values measured by UV differ slightly from the predicted values. This general agreement among the predicted and UV- and NMR-determined ΔH and

(11) (a) Breslauer, K. J.; Frank, R.; Blöcker, H.; Marky, L. A. *Proc. Natl. Acad. Sci. U.S.A.* **1986**, *83*, 3746. (b) Vesnaver, G.; Breslauer, K. J. *Proc. Natl. Acad. Sci. U.S.A.* **1991**, *88*, 3569.

(12) (a) Manning, G. S. *Q. Rev. Biophys.* **1978**, *11*, 179. (b) Record, Jr. M. T.; Mazur, S. J.; Melancon, P.; Roe, J.-H.; Shaner, S. L.; Unger, L. *Annu. Rev. Biochem.* **1981**, *50*, 997.

(13) Privalov, P. L.; Filimonov, V. V. *J. Mol. Biol.* **1978**, *122*, 447.

ΔS values for the native duplex suggests that the errors associated with these measurements are too small to account for the large difference in the enthalpy and entropy between the native and the modified duplex **1** (see the discussion below).

The Modified Duplex. By UV analyses, the modified duplex **1** shows a cooperative melting transition at both 10 and 100 μM; however, the melting temperature is reduced ~17 °C relative to the native duplex. At 2 mM, the NMR-detected thermal transitions of both duplex **1** and the native duplex are more cooperative, and the T_m of duplex **1** is 17 °C lower than that of the native duplex (Figure 2a). Each thymidine methyl reported the thermal transition, and more significantly, the difference in the thermodynamic values determined from T3-CH_3 and T4-CH_3 for the native and the modified duplex **1** were the same (Table 1). By this analysis, the overall decrease in stability of the modified duplex is seen to originate from two opposing factors: (i) a large decrease in enthalpy, 7 kcal mol^{-1}, and (ii) a favorable change in entropy of 15 eu mol^{-1}.

The positive charge in the backbone is expected to contribute enthalpic stabilization to duplex **1** due to the more favorable Coulombic interaction along the oligonucleotide backbone.[14a] The entropic contribution resulting from the counterion condensation on the modified backbone is expected to be unfavorable relative to its native analogue. Therefore, the observed changes in both ΔS and ΔH values between native and modified duplex **1** are in the opposite direction from those expected by electrostatic considerations. The *N*-acyl- and amide-linked hexamers of duplexes **2** and **3** were prepared as shown in Scheme 1 to remove the positive charge in the backbone. At a 5 μM duplex concentration in 1 M NaCl, the neutral backbone of the *N*-acyl duplex **2** showed no cooperative thermal melting transition. The *N*-acyl group in duplex **2** alters both the steric bulk of the linkage and the hybridization of the N atom; however, duplex stability was tolerant to substituents on the nitrogen atom at the corresponding position of an amide linkage when the group was changed from H to methyl to isopropyl.[2f,14b] Given the increased conformational flexibility of the ethylamine linkage of duplex **1** in comparison with the corresponding amide linkage in **3** (amide analogues **14a** to **14c** in Table 1 of ref 2f), the acyl substituent is expected to be well tolerated in **2.** Amide duplex **3** was prepared also, and its T_m of 14 °C, only slightly less than the T_m (18 °C) of the native DNA duplex, was consistent with the observation made by De Mesmaeker et al.[2f,14b] These data suggest that the positive charge is not the major factor contributing to duplex stability, and other factors should be sought to explain the overall destabilization of duplex **1** relative to the native structure.

Structural Analyses. Figure 3 shows the resonances of the exchangeable imino protons in 9:1 H_2O-D_2O for both the native DNA and the modified duplex **1**. All six of the expected protons are present in both structures, consistent with their participation in hydrogen bonding with the complementary strand. As the temperature is increased, the protons on the modified strand begin to exchange with solvent approximately 20 °C lower than do those in the native DNA. In both cases, fraying of the ends is followed by an apparent cooperative disruption of the internal base pairs.

These protons are assigned using the standard approach that follows the sequential connectivities involving exchangeable imino, amino, and adenine-H2 protons by 1D NOE difference spectra.[15] The 1D spectra made it possible to obtain a sufficient signal/noise ratio by accumulating many scans at the specific resonances (see the Materials and Methods). Figure 4 shows that irradiation of the imino proton of T4 results in two sharp H2 NOEs; a strong H2 NOE with its base-pairing partner A3 and a weaker H2 NOE with A4. Only one strong H2 NOE with A4 is observed when the imino proton of T3 is irradiated (Figure 4). These are characteristic of the Watson−Crick base-pairing motif in the B-form DNA duplex for both the native duplex (Figure 4a) and the modified duplex **1** (Figure 4b).[15a] To the extent that the Watson−Crick base-pairing motif is

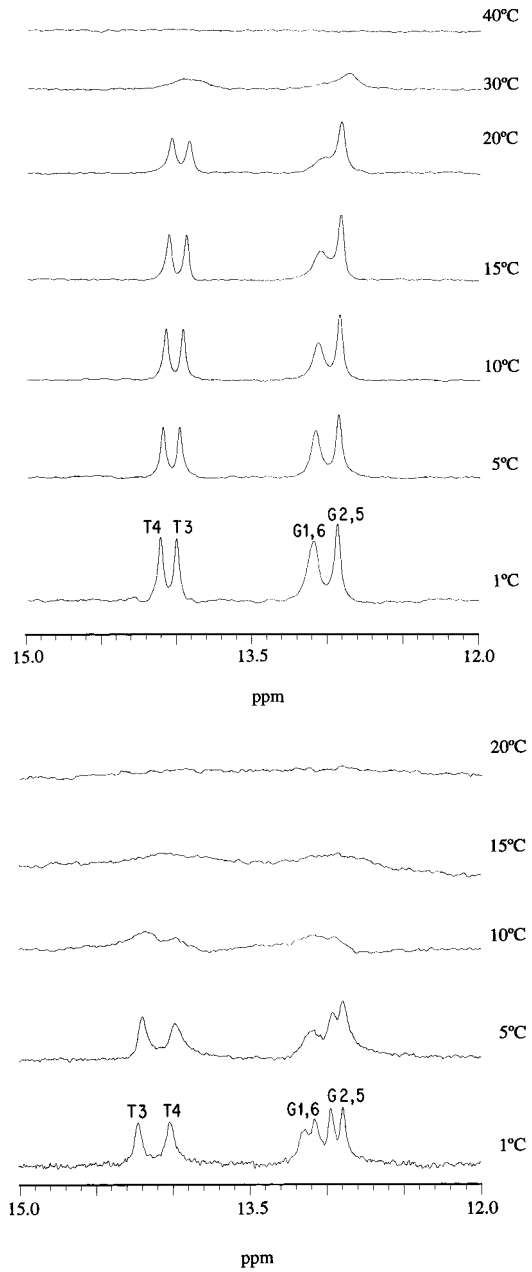

Figure 3. Temperature dependence of exchangeable imino proton resonances for (a, top) the native and (b, bottom). the modified duplex **1**. The exchange-out temperature of the hydrogen-bonded imino protons is higher by ca. 20 °C in the native duplex relative to the modified duplex **1**. The same samples as in Figure 2 are used, and the results are consistent with a ca. 17 °C difference in T_m between both duplexes shown in Figure 2a.

(14) (a) Dempcy, R. O.; Browne, K. A.; Bruice, T. C. *J. Am. Chem. Soc.* **1995**, *117*, 6140. (b) De Mesmaeker, A.; Waldner, A.; Lebreton, J.; Hoffmann, P.; Fritsch, V.; Wolf, R.; Freier, S. *Angew. Chem., Int. Ed. Engl.* **1994**, *33*, 226.

(15) (a) Chou, S. H.; Hare, D. R.; Wemmer, D. E.; Reid, B. R. *Biochemistry* **1983**, *22*, 3037. (b) Chou, S. H.; Flynn, P.; Reid, B. R. *Biochemistry* **1989**, *28*, 2435. (c) Weiss, M. A.; Patel, D. J.; Sauer, R. T.; Karplus, M. *Nucleic Acids Res.* **1984**, *12*, 4035.

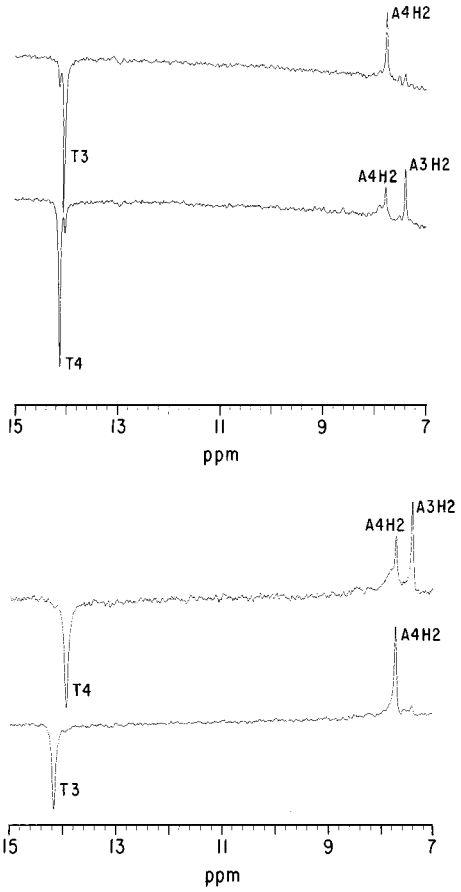

Figure 4. 1D NOE difference spectra showing the imino and AH2 proton connectivities for (a, top) the native and (b, bottom) the modified **1** DNA duplexes in the T3T4/A4A3 base pairs. Irradiation of the imino proton assigned to T4 results in two sharp H2 NOEs: a strong H2 NOE with its pairing partner A3 and a weaker H2 NOE with A4. Only one strong H2 NOE with A4 is observed when the imino proton of T3 is irradiated, consistent with a right-handed duplex. The NOE connectivities for imino and adenine H2 protons in the T3T4/A4A3 base pairs indicate that the Watson−Crick base-pairing motif is preserved in the backbone-modified DNA duplex **1**.

preserved in the native duplex, it is similarly maintained in the backbone-modified duplex **1**.

Characterization of the Modified Duplex Conformation via Nonexchangeable Protons. Figure 5a shows the characteristic NOESY cross-peaks for the sequence-specific connectivities between nonexchangeable base H8/H6 and sugar H2′/2″ protons in the modified DNA duplex **1**.[16] The solid lines show the sequence-specific assignments of the backbone-modified T_NT strand. Each base proton H8/H6 displays NOEs with its own and 5′-flanking sugar H2′/2″ protons and/or 3′-flanking methyl groups involving thymidine. Starting from the 5′-terminal nucleotide with only two NOEs of the 5′-base proton with its own sugar H2′/2″ protons, the sequential connectivities from base H8/H6 to sugar H2′/2″ protons were obtained across the entire strand without disruption. The dashed lines in Figure 5a show the corresponding assignments for the complementary native DNA strand in the modified duplex **1**.

The intranucleotide NOEs of H1′ and H3′ with H2′/2″ are utilized to distinguish the H2′ from H2″ protons on the basis of the variations in NOE cross-peak intensities. The NOE cross-peak intensity of H1′ with H2″ is stronger than with H2′ because the H1′−H2″ distance is usually shorter under all sugar pucker conformations. For the same reason, the corresponding NOE cross-peak intensity of the H3′ with H2″ is weaker than that of H3′ with H2′. On the basis of these criteria, the chemical shifts of H2′ and H2″ protons in the 3′-modified T3 sugar were assigned unambiguously even though their resonance frequencies are reversed in comparison with the usual order of H2′ and H2″ (Figure 5), except for the H2′ and H2″ protons of 3′-terminal G6 with a free 3′-OH group (Figure 5b). These assignments are important in defining the orientation of the methylene groups in the modified backbone with respect to the

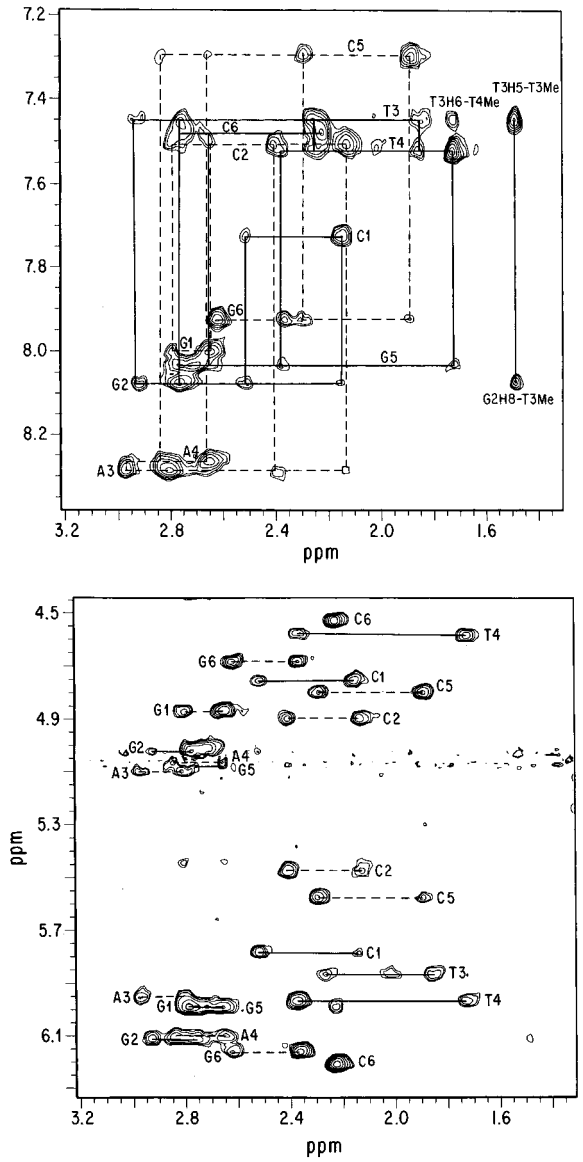

Figure 5. Expanded regions of the NOESY spectrum (D_2O, pH 6, 1 °C, 200-ms mixing time) showing (a, top) the sequence-specific connectivities between nonexchangeable base H8/H6 and sugar H2′/2″ protons for the modified DNA duplex **1**. The sequential connectivities for the d(CpGpT_NTpGpC) or TT strand and its complementary d(GpCpApApCpG) or AA strand are shown in solid and dashed lines, respectively, with the cross-peaks designated by the base and its sequence number. (b, bottom) NOE connectivities of the intranucleotide sugars H1′ and H3′ with their H2′/2″ protons in the modified DNA duplex **1**. The reversal in the chemical shift of H2′/2″ protons in T3 are revealed by a stronger cross-peak of the high-field signal with the T3-H1′ proton. The T3-H3′ proton is shifted upfield (see Figure 6) due to the chemical modification in the T3 sugar 3′ position.

(16) (a) Scheek, R. M.; Boelens, R.; Russo, N.; van Boom, J. H.; Kaptein, R. *Biochemistry* **1984**, *23*, 1371. (b) Wüthrich, K. *NMR of Proteins and Nucleic Acids*; Wiley & Sons: New York, 1984.

Table 2. Proton Chemical Shift Assignments for the Modified DNA Duplex 1 at pH 6, 1 °C[a]

residue	H6/H8	H5/CH_3	H1′	H2′	H2″	H3′	H4′	H5′/H5″	other
G1	8.01		5.99	2.63	2.79	4.87	4.27	3.73/3.73	
C2	7.51	5.43	5.48	2.13	2.40	4.90	4.18	4.12/4.10	
A3	8.30		5.96	2.81	2.97	5.10	4.35	4.15	AH2 7.43
A4	8.28		6.12	2.65	2.84	5.07	4.42	4.23	AH2 7.74
C5	7.30	5.29	5.59	1.89	2.30	4.80	4.16	4.26	
G6	7.93		6.17	2.62	2.36	4.68	4.21	4.08	
C1	7.73	5.92	5.79	2.15	2.51	4.75	4.11	3.76	
G2	8.09		6.11	2.78	2.91	5.01	4.26	4.14/4.06	
T3	7.46	1.49	5.86	2.27	1.86	2.78	4.05	4.42/4.27	C6′ 2.02; C7′ 3.39
T4	7.53	1.72	5.97	1.72	2.37	4.58	4.35	3.71/3.56	
G5	8.04		5.99	2.65	2.77	5.07	4.45		
C6	7.49	5.98	6.22	2.22	2.22	4.53	4.27	4.08	

[a] Referenced to TSP at 0.00 ppm.

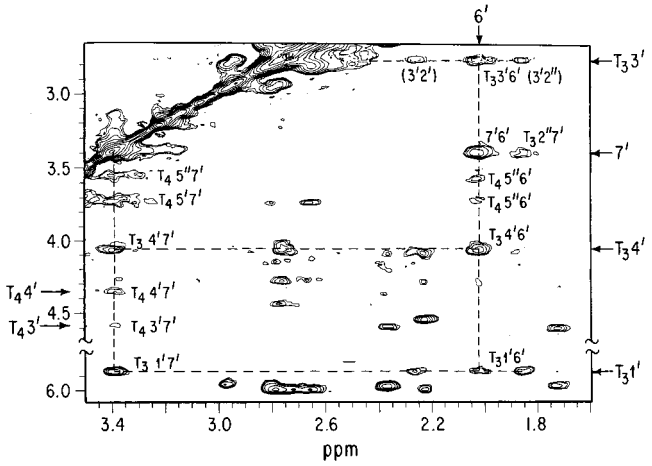

Figure 6. Expanded region of the NOESY spectrum (D_2O, pH 6, 1 °C, 200-ms mixing time) which highlights the cross-peaks of C7′ and C6′ methylene protons on the modified linkage with flanking sugar protons. Notice the stronger C7′−T3-H1′ cross-peak relative to those of C6′−T3-H1′ and even T3-H1′/H2″. The cross-peaks are assigned as the sugar protons and methylene groups are in Scheme 1.

T3 sugar ring. Figure 5b also indicates the chemical shift overlap for H2′ and H2″ in C6 as shown by a single strong cross-peak between H1′ and H3′ with H2′/2″, respectively.

The base-pairing scheme and sequential connectivities, with the uniformly much stronger NOEs of an intraresidue base proton with its own H2′/2″ protons than the corresponding NOEs with the 5′-flanking interresidue H2′/2″ protons across both strands, establish a canonical right-handed B-DNA conformation for the backbone-modified DNA duplex **1**.[16] The chemical shift assignments of the modified DNA duplex **1** are listed in Table 2.

NOEs of the Modified Linkage with Flanking Sugar Protons. The orientation of the phosphodiester linkage relative to the flanking nucleosides has eluded direct NOE observation in the DNA duplex due to the lack of protons and severe overlap of the 5′,5″ resonances.[17] The presence of the methylene units designated as C6′ and C7′ in the modified linkage of **1** permitted detailed analysis of the backbone geometry using the corresponding NOEs of these protons with the 5′-flanking sugar protons. These data are shown in a well-resolved region of the NOESY spectrum in Figure 6 and are summarized in Table 3 for the NOE cross-peaks of the C6′ and C7′ protons with the T3-H1′, -H2″, and -H4′ sugar protons underneath the T3 sugar ring. In contrast to the corresponding PO_2^- group that lies on the outside of the native duplex with maximal solvent accessibility, the C7′ CH_2 group in the modified duplex **1** can maintain close contact with the hydrophobic duplex interior and the T3 sugar ring. This orientation is supported by the stronger NOE cross-peak of T3-H1′−C7′ (H1′−C7′; ca. 2.7 Å) as compared to the T3-H1′−C6′ cross-peak (H1′−C6′; ca. 3.2 Å) and the NOE cross-peak of C7′ with T3-H2″ in Figure 6. In comparison, the corresponding distances of the O1P and O2P atoms of a PO_2^- group to the T3-H1′ proton, or H1′(i)−O1P(i + 1) and H1′(i)−O2P(i + 1), are 5.2−5.5 and 4.8−5.4 Å, respectively, in a canonical B-DNA conformation,[17,18] exceeding the detectable distance limit of the NOE (ca. 4.5−5.0 Å). An NOE cross-peak between the H1′ proton and a C7′ methylene has been observed in one other backbone modification (see Figure 9 in ref 17a), although it was suggested that the magnetization exchange may have occurred by spin diffusion in this case. The T3-H1′−C7′ cross-peak is indicative of an altered backbone orientation in duplex **1** as the presence of this cross-peak was confirmed in an NOESY spectrum collected at a 50-ms mixing time (see the Supporting Information), making spin diffusion unlikely as a major contributor to the observed cross-peaks.[19]

Table 3 tabulates proton−proton distances derived from NOE cross-peaks that are characteristic of the backbone conformation in the modified region. For comparison, the phosphate oxygen−proton distances in a native B-form DNA, but with a T3 sugar pucker in either C2′-endo or C3′-endo forms, are also listed. The difference between the distances of T3-H1′ to C7′ methylene of **1** and T3-H1′ to OP* of the native duplex is too large to be adequately accounted for by changes in the connecting sugar puckers (see Table 3). These data argue that the modified backbone of duplex **1** deviates significantly from the backbone conformation of the canonical DNA ensembles.

Structural Model. A preliminary structural model was derived by computer simulations with ca. 180 constraints derived from NMR experiments. A semiquantitative approach was taken to generate a 3D model using the Biosym software package.[20] The initial structure was built and modified from a B-DNA duplex using the Biopolymer and Builder modules in InsightII.[21] The energy minimization and dynamic simulations were carried out using the Discover module in InsightII with the CVFF force

(17) (a) Gao, X.; Brown, F. K.; Jeffs, P.; Bischofberger, N.; Lin, K.-Y.; Pipe, A. J.; Noble, S. A. *Biochemistry* **1992**, *31*, 6228. (b) Gao, X.; Jeffs, P. W. *J. Biomol. NMR* **1994**, *4*, 17.

(18) (a) Chandrasekaran, R.; Birdasall, D. L.; Leslie, A. G. W.; Ratcliff, R. L. *Nature* **1980**, *283*, 743. (b) Dickerson, R. E. *J. Mol. Biol.* **1983**, *166*, 419.

(19) Reid, B. R.; Banks, K.; Flynn, P.; Nerdal, W. *Biochemistry* **1989**, *28*, 10001.

(20) Dwyer, T. J.; Geierstanger, B. H.; Mrksich, M.; Dervan, P. B.; Wemmer, D. E. *J. Am. Chem. Soc.* **1993**, *115*, 9900.

(21) Arnott, S.; Hukins, D. W. L. *J. Mol. Biol.* **1973**, *81*, 93.

Table 3. Comparisons of the Proton−Proton Distance Derived from NOE Cross-Peaks Characteristic of the Backbone Conformation in the Modified Region with the Corresponding Phosphate Oxygen−Proton Distances in B-Form DNA but with the T3 Sugar Pucker in Either the C2′-endo or C3′-endo Conformation

i to *i* + 1[a]	H1′−OP* [b]	H2′−OP *	H2″−OP*	H3′−OP*	H4′−OP*
distances in B-DNA[c]	4.8−5.5	3.7−5.3	2.9−4.8	2.4−3.8	4.7
distances in twisted B-DNA[d]	4.7	3.8	2.5	3.9	2.8
T3 sugar to C7′ methylene	H1′−C7′	H2′−C7′	H2″−C7′	H3′−C7′	H4′−C7′
NOE derived distances[e]	2.7	∼4.5	3.2	>3.5	2.7
NOE cross-peaks at 50 ms	medium	null	weak	very weak	medium

[a] *i* and *i* + 1 refer to two consecutive residues. [b] OP* refers to the pseudo atom for two O1P and O2P atoms. [c] Distance ranges for B-DNA were taken from Table 4 in ref 17a. [d] The twisted B-DNA represents the extreme case of the T3 sugar pucker switching from normal C2′-endo to C3′-endo. [e] The NOE-derived distances were obtained using the integration of the NOE cross-peak at 50-ms and 200-ms mixing times; the NOE cross-peak intensities at 50-ms mixing time provided the control on the distance estimates.

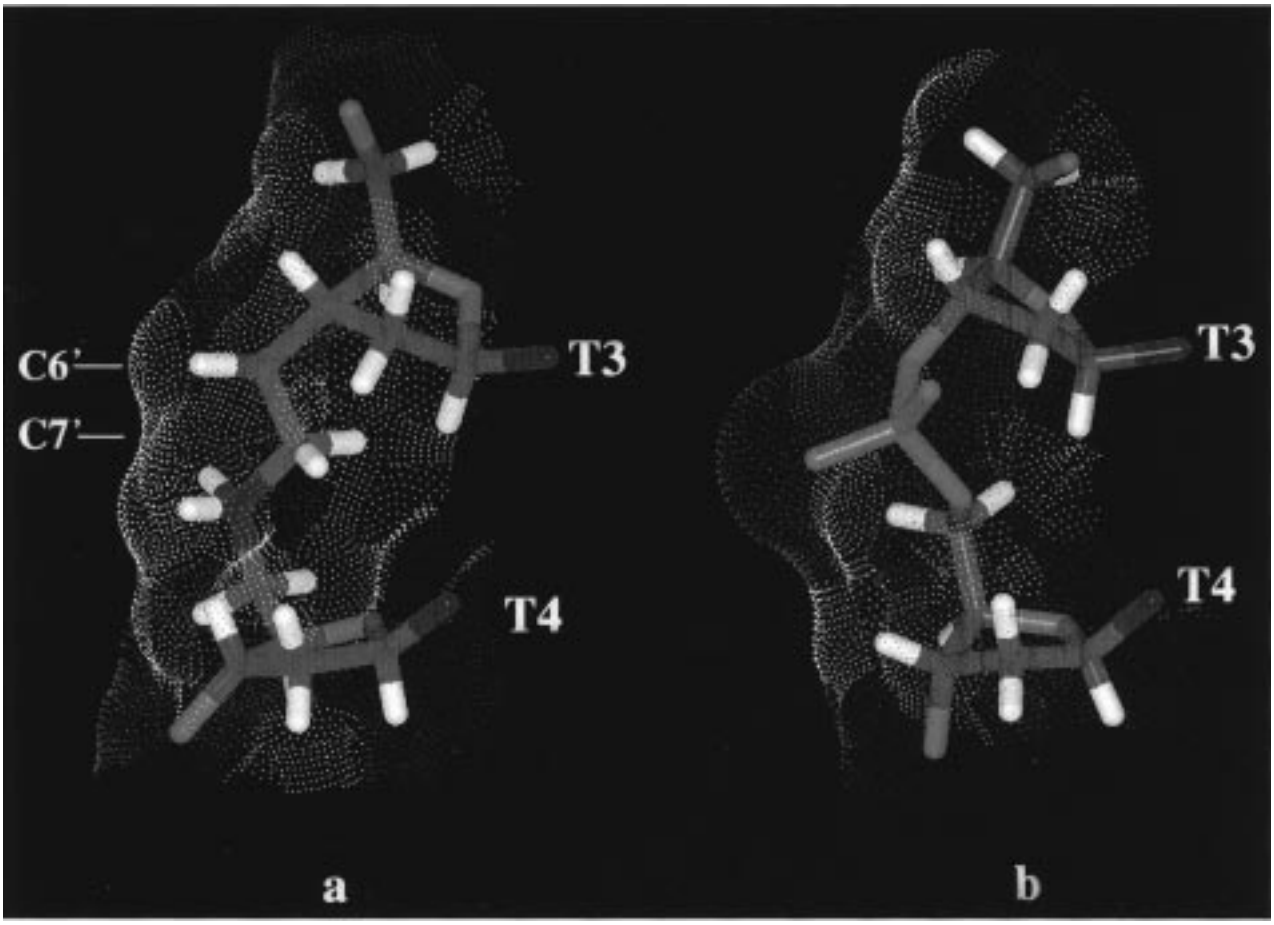

Figure 7. Comparison of structures with their solvent-accessible surfaces (dots) in the TT region of (a) the ethylamine-containing strand, and (b) its native counterpart in B-form DNA. Both strands were cut out of the full duplexes, generated from crystal structure data for (b) and from molecular dynamics simulations incorporating NMR constraints for (a). The intruding C7′ methylene with the flat solvent-accessible surface in the modified linkage **1** contrasts markedly with the maximally solvent-accessible phosphate of the phosphodiester linkage.

field parameters. The hydrogen bonds in the Watson−Crick base pairs were constrained as supported by the imino proton experiments to prevent the two strands from breaking apart during simulations. The simulations were started by using the simulated annealing protocol to satisfy local NOE constraints in the TT dimer region while the rest of the structure was constrained. Once the NOE constraints in the TT dimer region were satisfied, the whole structure was refined to remove steric clashes with all experimental constraints using dynamic calculations and energy minimization to generate the preliminary 3D model. It should be pointed out that DNA is an extended, nonglobular molecule, and NMR can only provide short-range NOE distance constraints (<4.5 Å). Given no direct long-range experimental constraints, we refrain from inferring any changes in the global structural features of the derived DNA model, focusing instead on the local structure in the modified TT dimer region where the extensive NOEs are available for constraining structures. Figure 7a highlights the TT dimer region from the calculated structure model next to the corresponding region in the native B-DNA[21] duplex in stick model representation, Figure 7b. The solvation surfaces were created by rolling a water molecule of 1.4 Å radius over the van der Waals surfaces of the molecule.[22] As constrained by the NMR data, the hydrophobic C7′ methylene unit has swung from the usual solvent-exposed position of the PO_2^- group into the interior of the double helix, in close contact with a core formed by the base edges and sugar rings of the flanking TT/AA nucleosides. We simply refer to this region as the hydrophobic core of a DNA

(22) Alden, C. J.; Kim, S.-H. *J. Mol. Biol.* **1979**, *132*, 411.

duplex although it is certainly more extended than the core of a globular protein.

Discussion

The structural and thermodynamic analyses of duplex **1** have been compared to those of an unmodified DNA duplex of the same sequence. The destabilizing effect of the modification may be the result of duplex destabilization, stabilization of the backbone-modified single strand, or both. Because the nearest-neighbor data are derived from measurements in which the single-stranded oligonucleotides are in the random coiled state, the good agreement between the observed and predicted values of ΔH for the native duplex (Table 1) argues that there is no single-stranded structure that contributes to the observed ΔH and ΔS values on duplex formation.[11b] Indeed, a direct calorimetric measurement[11b] has shown that the thermodynamic contribution of the structured single-stranded DNA makes the observed ΔH value of duplex formation significantly lower than the predicted value using nearest-neighbor data.[11a]

The NMR data provide complementary evidence supporting the observed change in stability being attributable to the duplex. The difference between the $\Delta\delta$ values of the T3-CH_3 groups in duplex **1** and its native analogue is 0.04 ppm, and the $\Delta\delta$ values converge in the thermally unfolded strands. This convergence of the chemical shift values suggests that the T3-CH_3 probe is responsive to the local change in duplex **1** rather than to the chemical modification, and therefore, duplex destabilization, rather than a structured single strand, is the primary contributor to the observed thermodynamic difference between duplex **1** and the native DNA.

Although an overall B-DNA structure with base stacking and interstrand H-bonds was clearly present in duplex **1**, a global destabilization of duplex **1** relative to its native duplex is detected by both UV and NMR monitored thermal unfolding experiments. This destabilization is reflected in an unfavorable change in ΔH of 7 kcal mol^{-1} (Table 1).

A significant conformational change in the backbone of duplex **1** was detected by the NMR experiments. This structural change is of particular interest in relation to the significant entropic stabilization. A 15 eu mol^{-1} change in entropy is significant; sequence-dependent variations in ΔS are typically less than 3 eu mol^{-1} per base pair.[11a] Modifying the phosphodiester into the neutral ethyl phosphotriester gives a similar positive entropic change, but only of $\sim$7 eu mol^{-1} per modification.[23] Given the extensive cooperativity in forming a DNA duplex, it is likely that this local change near the modified backbone could cause a global weakening in the stability of duplex **1**. Therefore, both the direction and magnitude of the changes in ΔH and ΔS and their correlation with the structural change in the backbone of the duplex **1** deserve further consideration.

Factors Contributing to the Observed Difference in ΔS. The factors that contribute to the change in entropy can be expressed by eq 7. The $\Delta S_{\text{conformation}}$ has been estimated by the

$$\Delta S_{\text{observe}} = \Delta S_{\text{conformation}} + \Delta S_{\text{ion-condensation}} + \Delta S_{\text{other}} \qquad (7)$$

expression nR ln 3 where R is the gas constant and n is the number of bonds per residue along the backbone.[24] Each bond can populate three conformers in the random strand, but only one upon duplex formation. To account for the observed difference in ΔS exclusively as a function of conformational differences would require a difference of approximately seven bonds along the DNA backbone between the native and modified duplex, or $7 \times 1.987 \ln 3 = 15$ eu mol^{-1}. Although the ethylamine linker may be more flexible than the phosphodiester linkage,[2e,f] the number of backbone bonds in duplex **1** has not been changed and the observed difference in ΔS is too large to be explained by the change in the conformational entropy of the modified backbone.

With respect to ion condensation, the replacement of a phosphate group with a positively charged ethylamine should reduce the net charge density along the modified backbone. The entropic driving force resulting from the counterion condensation on the modified DNA backbone would become less favorable to duplex formation rather than more favorable. With respect to hydration, high-resolution X-ray diffraction data from Dickerson and co-workers reveal the presence of a spine of H_2O molecules in the minor groove of A−T base pairs[25] and the dT·dA duplex appears to have an even higher degree of hydration.[26] Breslauer and co-workers[27] have attempted to interpret the thermodynamic data for DNA bending drug interactions in terms of the disruption of levels of DNA hydration beyond the minor groove. The increase in entropy appeared to correlate with the release of the tightly bound water molecules into the bulk medium resulting from the structural transition and/or ligand binding. We have no direct experimental evidence that identifies the change in water binding in the modified backbone even though such a disruption is expected in the modified dAdT region and might contribute to the observed increase in ΔS.[5] On the other hand, an entropic factor has been identified by studying the duplex formation of a DNA hexamer in 10 mol % alcohol−water mixtures.[8c] The overall destabilization upon introduction of alcoholic cosolvents to the DNA solution is attributed to an unfavorable change in entropy that ranges from 7 (in MeOH) to 20 (in PrOH) eu mol^{-1} (see Table 3 in ref 8c). This change is consistent with a contribution from nonspecifc hydrophobic interactions to stabilizing the DNA duplex; the entropic driving force is disrupted upon adding alcohols. Incidently, this change in ΔS is of the same magnitude as we have observed here, suggesting that changes in the hydrophobic interaction from the native to the modified duplex **1** might be invoked to explain the significant and favorable change in ΔS, even though only one backbone linkage is modified in duplex **1**.

Collapse of the Modified Backbone onto the Hydrophobic Interior of the DNA Duplex. The NMR analysis showed that the C7′ methylene replacing the PO_2^- group can reside in close contact with a core formed by the base edges and sugar rings of the connecting nucleotides. The structural change shown in Figure 7 is consistent with a partitioning of the flexible ethylamine onto the hydrophobic core of this duplex. Hydrophobic collapse is a term frequently invoked to describe the folding of proteins,[28] but is not commonly applied to nucleic acids. This interpretation nevertheless seems valid in this case for several reasons.

The structures of nucleic acids display the protein folding pattern of "polar out, nonpolar in". The polyanionic phosphate groups are exposed to water, and the hydrophobic moieties of

(23) Pless, R. C.; Ts'o, P. O. P. *Biochemistry* **1977**, *16*, 1239.
(24) (a) Privalov, P. L. *Adv. Protein Chem.* **1979**, *33*, 167. (b) Baldwin, R. L. *Proc. Natl. Acad. Sci. U.S.A.* **1986**, *83*, 8069. (c) Luo, P.; Lynn, D. G. Submitted for publication.
(25) Drew, H. R.; Dickerson, R. E. *J. Mol. Biol.* **1981**, *151*, 535.
(26) Pilet, J.; Blicharski, J.; Brahms, J. *Biochemistry* **1975**, *14*, 1869.
(27) (a) Breslauer, K. J.; Remeta, D. P.; Chou, W.-Y.; Ferrante, R.; Curry, J.; Zaunczkowski, D.; Snyder, J. G.; Marky, L. A. *Proc. Natl. Acad. Sci. U.S.A.* **1987**, *84*, 8922. (b) Marky, L. A.; Breslauer, K. J. *Proc. Natl. Acad. Sci. U. S.A.* **1987**, *84*, 4359.
(28) Kim, P. S.; Baldwin, R. L. *Annu. Rev. Biochem.* **1990**, *59*, 631.

Scheme 3. A Model for the Altered Stability of Modified Duplex **1**[a]

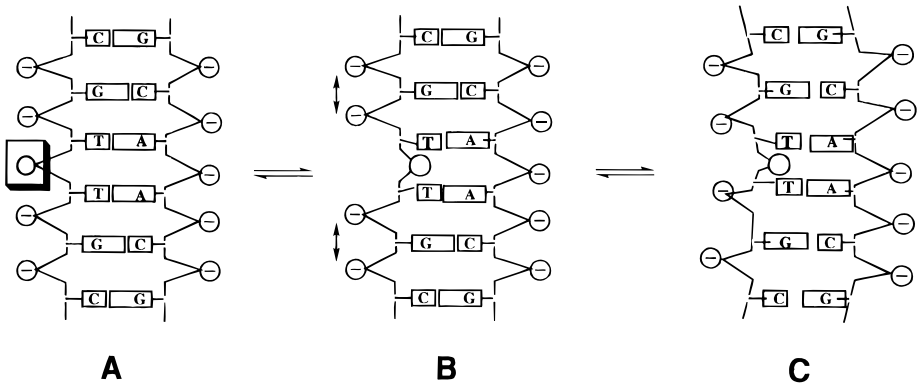

[a] The duplex with the negatively charged phosphate removed (**A**) initiates the collapse of the ethyl amine onto the hydrophobic interior of the duplex (**B**). The two flanking phosphates are forced to reduce the distance separating them, causing backbone curvature and loss of the optimal geometry for base-stacking and H-bonding interactions (**C**).

the bases and sugars are buried inside. Estimation of the solvent-accessible surface has shown that two-thirds of the hydrophobic surfaces are buried upon duplex formation, while the phosphate groups account for almost half of the surface exposed to the solvent[22] and are maximally partitioned into water.[25,29] Further, examination of the DNA duplex structure shows that the positions occupied by the PO_2^- and the 5′-O on the backbone linkage are flexible, being able to rotate without causing undue constraints on base pairing and sugar pucker geometry. In contrast, conformational degrees of freedom in both the 3′-O and 5′-methylene positions along the backbone are primarily determined by the sugar pucker of the connecting nucleotides. Indeed, the X-ray structure of a single backbone-modified DNA with the O atom at the 3′-O position replaced by a methylene group is essentially identical to the B-form conformation of the native DNA duplex.[30] It follows that the C6′ methylene in the modified duplex **1** could be accommodated in a conformation similar to that of the corresponding O atom in the native DNA duplex (Figure 7a). Therefore, the spatial orientation of any chemical group at the unrestricted position of the phosphate, or the C7′ methylene in duplex **1**, should be determined by partitioning between the solvent-exposed surface and the solvent-shielded hydrophobic interior.

Estimates of the Magnitude of the Hydrophobic Interaction. Using in vitro selection experiments, the magnitude and specificity of the hydrophobic interaction between aliphatic groups with the interior of RNA have been directly estimated.[31] The binding free energy per methylene is up to 1.5 kcal mol^{-1} at 25 °C, comparable to the similar interaction in proteins. Because the hydrophobic interaction is entropy-driven at room temperature,[24b] ΔS values of transferring one CH_2 group from a water-exposed site into the hydrophobic interior of nucleic acids can be 5 eu mol^{-1}, or up to 10 eu mol^{-1} for the two CH_2 groups in duplex **1**, a significant percentage of the observed difference in ΔS between the native and the modified duplex **1** (Table 1).

Despite their positive charge, amines, like alcohols, are considered soluble hydrocarbons because their thermodynamic properties in dilute aqueous solution are controlled predominantly by the aliphatic groups. A large and positive change in heat capacities and negative change in entropy are observed upon transferring from the vapor state to infinitely dilute aqueous solutions;[32a] the change in ΔS is -42.2 eu mol^{-1} for ethylamine, -39.8 eu mol^{-1} for ethanol, and -33.6 eu mol^{-1} for ethane at 25 °C, respectively.[32] After the change in entropy due to vaporization at 25 °C has been corrected, the change in ΔS from the liquid state to an infinitely dilute aqueous solution for ethanol is -7 eu mol^{-1}. Alternatively, using the liquid hydrocarbon model,[24b,c] the $\Delta C_p = 33.9$ eu mol^{-1} for transfer of pure ethanol to an aqueous solution at infinite dilution at 25 °C,[33] the corresponding change in ΔS is equal to $\Delta C_p \ln(T/T_s)$ or -9 eu mol^{-1}, where $T_s = 386$ K for the reference temperature in the liquid hydrocarbon model.[24b] Both of these estimates are of magnitude and direction similar to those seen with the RNA measurements and close to the observed 15 eu mol^{-1} attributed to the hydrophobic collapse of the ethylamine group onto the interior of the DNA duplex. The hydrophobic interaction between the ethylamine linkage and the hydrophobic core formed by the sugar rings and base edges appears to be a significant contributor to the change in ΔS of duplex **1**.

Local Backbone Distortion and Structural Stability of the Modified Duplex. Due to the intrinsic difficulty in describing cooperativity involving long-range interactions underlying the folding properties of biopolymers such as proteins,[28] a model based on the cooperativity of the DNA duplex stability is required to relate the local backbone distortion, which is detected by NMR and assigned to a favorable change in ΔS, to the overall destabilization of the modified duplex **1**. Scheme 3 suggests that a duplex containing a more hydrophobic linkage (**A**) initiates the conformational partitioning onto the hydrophobic interior of the duplex (**B**). This movement accentuates the gap between the two flanking phosphates, forcing a movement to shorten their intervening distance and destabilizing the optimal geometry for duplex stability (**C**).

The driving force for the movement of these phosphates could have several origins. It has been demonstrated recently that asymmetric charge neutralization of DNA phosphate groups can result in the bending of the DNA duplex around the site of neutralization.[34] We suggest that another mechanism, namely, the collapse of a hydrophobic linkage such as C7′ methylene of duplex **1**, can also contribute to the bending of the DNA duplex. The positive charge could also act in concert with the

(29) Saenger, W. *Principles of Nucleic Acid Structure*; Springer-Verlag: New York, 1984.

(30) Heinemann, U.; Rudolph, L.-N.; Claudis, A.; Morr, M.; Heikens, R. F.; Blocker, H. *Nucleic Acids Res.* **1991**, *19*, 427.

(31) Majerfeld, I.; Yarus, M. *Nature Struct. Biol.* **1994**, *1*, 287.

(32) (a) Franks, F., Reid, D. S. In *Water*; Franks, F., Ed.; Plenum Press: New York, 1973; Vol 2, Chapter 5, pp 323−404. (b) Frank, H. S.; Evans, M. W. *J. Chem. Phys.* **1945**, *13*, 507.

(33) Alexander, D. M.; Hill, D. J. T. *Aust. J. Chem.* **1969**, *22*, 347.

(34) (a) Strauss, J. K.; Maher III, L. J. *Science* **1994**, *266*, 1829. (b) Strauss, J. K.; Roberts, C.; Nelson, M. G.; Switzer, C.; Maher, L. J., III. *Proc. Natl. Acad. Sci. U.S.A.* **1994**, *93*, 9515.

hydrophobic collapse by pulling the two flanking phosphates of the same strand together, although the *N*-acyl duplex **2** argues that the positive charge in the duplex **1** might stabilize duplex **1** relative to **2**, possibly by a Coulombic attraction with the interstrand phosphates. The neutral amide **3** is significantly stabilized, and this stability can be assigned to the reduced flexibility of the amide and the resulting inability of this linker to partition onto the hydrophobic core. The local distortion is proposed to disrupt the cooperativity in forming a duplex, causing backbone curvature, a loss of the optimal geometry for base-stacking and H-bonding interactions, and resulting in the general loss in the enthalpic stabilization of duplex **1**.

Conclusions

In this work we have analyzed the structural and thermodynamic properties of the backbone modified DNA duplex **1** by comparing the native duplex with **1**, **2**, and **3**. A concern in making this comparison is that the physical factors which control the stability of a modified duplex may vary from one modification to another and chemical modifications, such as removal of a single phosphate, can introduce factors other than those intrinsic to the native duplex. We posed five questions that we saw as central to the studies of backbone-modified oligonucleotide analogues and have developed them for this comparison.

Both structural and thermodynamic evidence supports the use of a two-state model in analyzing the thermal unfolding of a duplex with a single structural change in the center of one strand. This structural change destabilizes the duplex. While the effect of charge is analyzed qualitatively by referring to the properties of chemical analogues **2** and **3** as well as data from the literature,[2e,f] a more quantitative or semiquantitave approach is taken in the analysis of the change in entropy due to solvation and the hydrophobic nature of the modification. The favorable change in ΔS has been assigned to the hydrophobic nature of the ethylamine linkage, and the unfavorable change in ΔH is due to the more global disruption of H-bonding and stacking interactions. This effect is best summarized in a model that takes into account how a local backbone distortion might couple with long-range interactions in determining DNA duplex formation.[34] This model highlights a fundamental property underlying the folding of biopolymers: a single modification in the DNA backbone can result in favorable changes in entropy and, at the same time, alter the overall duplex stability by disrupting the cooperativity of the folding process. This study of a single modification provides the groundwork and prospective necessary for understanding and designing the more extensively modified structures necessary for metabolically stable antisense reagents.

This model has proven to be of value in the design and characterization of systems for template-directed synthesis. The backbone-modified structures have increasingly underscored the role played by the phosphates in preorganizing the nucleic acids into an extended conformation. This preorganization appears to be an important structural contributor in driving efficient strand recognition and duplex formation.[6] The rigidity of the imine precursor to duplex **1** has now been exploited in preparing the smallest catalytic nucleic acid that efficiently gives catalytic turnover and reduces production inhibition.[5] It is now possible to better consider other ligation and polymerization reactions that can be used to extend this general concept of translating information from a DNA polymer into other polymeric analogues.

Materials and Methods

Synthetic Procedures. General methods as well as detailed procedures for the construction of **4**−**7** are provided in the Supporting Information.[35−40]

Bis-*O*-*t*-BDMS-5′-thymidinylaminoethylthymidine (8). 3′-Carboxyaldehyde-5′-OTBDMS-3′-deoxythymidine (**5**) (281 mg, 740 μmol)- and 5′-amino-3′-OTBDMS-5′-deoxythymidine (**7**) (314 mg, 880 μmol, 1.2 equiv) were dissolved in 3 mL of freshly distilled THF, and 233 mg (1.1 mmol, 1.5 equiv) of sodium cyanoborohydride[41] was added with stirring at room temperature. TLC indicated that reaction was complete within approximately 2 h (TLC; 9:1 $CHCl_3$−MeOH; R_f = 0.25). The reaction solution was concentrated and chromatographed on silica gel (9:1 $CHCl_3$−MeOH) to yield a white foam, 504 mg (700 μmol, 95%). ^{1}H NMR (300 MHz, $CDCl_3$/TMS): δ = 7.58 (d, J = 1 Hz, 1H, H-6); 7.17 (d, J = 1 Hz, 1H, H-6); 6.12 (t, J = 6.2 Hz, 1H, H-1′); 6.06 (dd, J = 4.1 Hz, 6.3 Hz, 1H, H-1′); 4.30 (m, 1H, H-3′b); 4.00 (dd, J = 2.9 Hz, 12.3 Hz, 1H, H-5′a); 3.92 (m, 1H, H-4′b), 3.73 (m, 2H, H-4′a, H-5″a); 2.8−2.9 (m, 2H, H-5′/5″b) 2.72 (t, J = 7.3 Hz, 2H, H-7′/7″a); 2.1−2.3 (m, 7H, H-6′/6″a, H-2′/2″a, H-2′/2″b, H-3′a); 1.93 (d, J = 1 Hz, 6H, thymine-CH_3); 0.93, 0.89 (s, 18H, (CH_3)$_3$CSi); 0.11, 0.08 (s, 12H, (CH_3)$_2$Si). ^{13}C NMR (75 MHz, $CDCl_3$): δ = 164.4, 164.1 (C-4a,b); 150.7, 150.6 (C-2a,b); 136.1, 135.8 (C-6); 111.3, 110.3 (C-5a,b); 86.6, 85.4 (C-4′a,b); 85.4, 85.3 (C-1′a,b); 72.8 (C-3′a); 63.1 (C-5′a); 51.3 (C-7′a); 48.7 (C-5′); 40.5, 39.4 (C-3′a, C-2′b); 35.7 (C-6′a); 32.8 (C-2′a); 26.2, 25.9 ((*C*H$_3$)$_3$CSi a,b); 18.7, 18.1 ((CH$_3$)$_3$*C*Si, a,b); 12.8 (thymine-*C*H$_3$ a,b); −4.5, −4.6, −5.1 ((*C*H$_3$)$_2$Si a,b).

Bis-*O*-*t*-BDMS-5′-thymidinyl-*N*-acetylaminoethylthymidine (9). Triethylamine (112 mg, 1.1 mmol, 20 equiv), acetic anhydride (22.5 mg, 220 μmol, 4 equiv), and bis-*O*-*t*-BDMS-5′-thymidinylaminoethylthymidine (**8**) (40 mg, 55 μmol) were dissolved in 2 mL of dichloromethane. The reaction was complete in 1 h as determined by TLC (EtOAc, R_f = 0.18; 9:1 $CHCl_3$−MeOH, R_f = 0.43). Concentration of the solvent gave **9** as a colorless oil in quantitative yield. NMR analysis indicated the presence of the two *N*-acetate rotamers in approximately equal amounts. ^{1}H NMR (400 MHz, $CDCl_3$/TMS): δ = 9.66, 9.38, 9.31 (3s, 2H, NHa,b); 7.61, 7.56, 7.23, 7.00 (4s, 2H, H-6′); 6.15 (t, J = 6.7 Hz, 0.5H, H-1′a); 6.07 (m, 1H, H-1′b); 5.87 (dd, J = 5 Hz, 8 Hz, 0.5H, H-1′a); 4.31 (m, 1H, H-3′b); 3.99 (m, 2H, H-4′a, H-5′a); 3.75 (m, 2H, H-4′b, H-5″a), 3.43 (m, 4H, H-7′/7″a, H-5′/5″b); 2.5 (m, 1H, H-3′a); 2.25 (m, 4H, H-6′/6″a, H-2′a, H-2′b); 2.1 (m, 2H, H-2″a, H-2″b); 2.10, 2.13 (s, 3H, (CH_3)C(O)N); 2.06, 1.96, 1.94, 1.93 (s, 6H, thymine-CH_3); 0.94, 0.93 (s, 9H, (CH_3)$_3$CSi); 0.91 (s, 9H, (CH_3)$_3$CSi); 0.14, 0.13, 0.12, 0.11, 0.10, 0.91 (s, 12H, (CH_3)$_2$-Si). ^{13}C NMR (75 MHz, $CDCl_3$): δ = 170.8, 170.7 ((*C*H$_3$)C(O)N); 164.4, 164.3, 164.2 (C-4a,b); 150.9, 150.7, 150.6, 150.2 (C-2a,b); 137.6, 137.5, 136.5, 135.9 (C-6a,b); 111.4, 110.5, 110.4 (C-5a,b); 88.3−85.3 (8s, C-4′a,b; C-1′a,b); 73.8, 72.9 (C-3′b); 63.2, 62.8 (C-5′a); 51.2 (C-7′a); 47.8, 47.3 (C-5′a); 39.7, 39.6, 39.5, 39.1 (C-3′a, C-2′b); 35.4, 35.2 (C-6′a); 31.5, 30.4 (C-2′a); 26.1, 25.9 ((*C*H$_3$)$_3$CSi a,b); 22.0, 21.5 ((*C*H$_3$)C(O)N 18.6, 18.1 ((CH$_3$)$_3$*C*Si, a,b); 12.8, 12.7 (thymine-*C*H$_3$ a,b); −4.3, −4.5, −4.7, −5.2 ((*C*H$_3$)$_2$Si a,b).

Amide Dimer 10. 5′-OTBDMS-3′-deoxythymidine-3′-acetic acid (**6**) (100 mg, 250 μmol) and 5′-amino-3′-OTBDMS-5′-deoxythymidine (**7**) (100 mg, 270 μmol, 1.1 equiv) were dissolved in 5 mL of dichloromethane. 4-(Dimethylamino)pyridine (Fisher; 16 mg, 130 μmol, 0.5 equiv) and *p*-toluenesulfonic acid (15 mg, 80 μmol, 0.3 equiv) were added, followed by 1-(3-(dimethylamino)propyl)-3-ethylcarbodiimide·HCl (58 mg, 300 μmol, 1.2 equiv). The reaction solution was

(35) Ogilvie, K. K. *Can. J. Chem.* **1973**, *51*, 3799.
(36) (a) Prisbe, E. J.; Martin, J. C. *Synth. Commun.* **1985**, *15*, 401. (b) Fiandor, J.; Tam, S. Y. *Tetrahedron Lett.* **1990**, *31*, 597.
(37) Keck, G. E.; Enholm, E. J.; Wiley: M. R. *Tetrahedron* **1985**, *41*, 4079.
(38) Chu, C. K.; Doboszewski, B.; Schmidt, W.; Ullas, G. V. *J. Org. Chem.* **1989**, *54*, 2767.
(39) Demuth, M.; Ritterskamp, P.; Weigt, E.; Schaffner, K. *J. Am. Chem. Soc.* **1986**, *108*, 4149.
(40) Yamamoto, I.; Sekine, M.; Hata, T. *J. Chem. Soc. Perkin Trans. 1* **1980**, 306.
(41) Borch, R. F.; Bernstein, M. D.; Durst, H. D. *J. Am. Chem. Soc.* **1971**, *93*, 2897.

stirred at room temperature for 2 h, whereupon TLC indicated the reaction was complete. Dilution with chloroform and washing with water were followed by concentration of the organic layer and flash chromatography (EtOAc; $R_f = 0.21$) to yield 125 mg (170 μmol, 68%) as a slightly yellow oil. See ref 42 for independent syntheses of this linkage. ^{1}H NMR (400 MHz, $CDCl_3$/TMS): δ = 9.47, 9.29 (2 br s, 2H, thymine-NH a,b); 7.59 (d, J = 1 Hz, 1H, H-6); 7.07 (m, 1H, C(O)-NH); 7.02 (s, 1H, H-6); 6.25 (t, J = 6.5 Hz, 1H, H-1′a); 5.68 (t, J = 6.8 Hz, 1H, H-1′b); 4.40 (dt, J = 4.5 Hz, 7.1 Hz, 1H, H-3′b); 3.93 (m, 2H, H-4′b, H-5′a); 3.81 (m, 1H, H-4′a); 3.75 (dd, J = 2.8 Hz, 11.3 Hz, H-5″a); 3.67 (ddd, J = 4.8 Hz, 6.6 Hz, 14.2 Hz, 1H, H-5′b); 3.46 (dt, J = 3.5 Hz, 14.2 Hz, 1H, H-5″b); 2.83 (m, 1H, H-3′a); 2.64 (dt, J = 6.7 Hz, 13.5 Hz, 1H, H-2′b); 2.4 (m, 2H, H-6′/6″a); 2.1−2.25 (m, 3H, H-2″b, H-2′/2″a); 1.93, 1.91 (s, 6H, thymine-CH_3); 0.93, 0.88 (s, 18H, (CH_3)$_3$CSi); 0.13, 0.12, 0.07, 0.08 (s, 12H, (CH_3)$_2$Si). ^{13}C NMR (75 MHz, $CDCl_3$): δ = 171.5 (C-7′a); 164.4 (C-4a,b); 151.2, 150.6 (C-2a,b); 138.7, 135.9 (C-6a,b); 111.2 (C-5a,b); 89.8 (C-4′a,b); 85.6, 84.8 (C-1′a,b); 72.4 (C-3′b); 64.5 (C-5′a); 40.5 (C-5′b); 39.7, 39.5 (C-3′a, C-2′b); 37.8 (C-6′a); 36.1 (C-2′a); 26.1, 25.9 ((*C*H$_3$)$_3$CSi a,b); 18.0 ((*C*H$_3$)$_2$Si a,b); 12.7, 12.5 (thymine-*C*H$_3$ a,b); −4.6, −4.7, −5.2 ((*C*H$_3$)$_2$-Si a,b).

DNA Hexamers. The same procedure was followed for elaboration of each dimer into oligonucleotides. The bis-silylated dimer was deprotected overnight with excess tetrabutylammonium fluoride (1 M in THF, Aldrich) followed by flash chromatography. Yields of this deprotection were commonly in the 50−80% range. Removal of residual tetrabutylammonium salts proved to be difficult, so other methods of deprotection are currently under investigation.[43]

Desilylation was followed by dimethoxytritylation at the 5′-alcohol. This protection was carried out overnight in anhydrous pyridine with 1.5 equiv of DMTrCl. Yields after chromatography were approximately 70%. Conversion to the phosphoramidite was performed as follows: The tritylated dimer was dissolved in freshly distilled THF along with diisopropylethylamine (3 equiv). 2-Cyanoethyl *N*,*N*-diisopropylchlorophosphoramidite (1.5 equiv) was added and the reaction stirred under nitrogen at room temperature. TLC indicated the reaction was complete within approximately 1 h; this solution was rapidly chromatographed on silica. Concentration was accomplished by repeated coevaporation with heptane and acetonitrile. Following overnight evacuation on a vacuum pump, the phosphoramidite dimer was used in solid-phase DNA synthesis of the hexamer.

Solid-Phase Hexamer Synthesis. Solid-phase synthesis of the modified hexamers was carried out on an ABI 380B automated synthesizer by Paul Gardner of the University of Chicago Oligonucleotide Synthesis Facility on scales ranging from 3 to 9 μmol. Production of the trityl cation at the deprotection step after addition of the modified dimer indicated successful coupling to the growing chain. Synthetic oligonucleotides were purified as follows: following cleavage from the solid support, the fully deprotected oligonucleotide was subjected to cation-exchange chromatography (Dowex 50 × 2−100, Na^+ form). The oligonucleotides were prepurified by low-pressure reversed-phase chromatography (C_{18} Sep-Pak, Waters) and then purified for UV melting curves by semipreparative HPLC using a gradient of ammonium acetate in a mixture of 20% acetonitrile and 80% 20 mM aqueous sodium phosphate on a DuPont Zorbax Oligo column. NMR quantities were purified through a Sephadex G-10 column with 10 mM NH_4HCO_3 buffer solution. The volatile salts were removed by repeated lyophilization.

NMR Sample Preparation. DNA samples were exchanged into their sodium form by passing through an ion-exchange column of a Dowex 50 × 2−100 resin (Aldrich) versus NaOH. The lyophilized samples were eluted through a Sep-Pak C18 column with a gradient of 0−6% acetonitrile in water, and were finally purified through a Sephadex G-10 column with 10 mM NH_4HCO_3 buffer solution. The volatile salts were removed by repeated lyophilization. Concentrations of DNA oligomers were determined by their UV absorbances at 260 nm, and the molar extinction coefficients were calculated to be 5.98 × 10^4 M^{-1} cm^{-1} for d(GCAACG) and 5.10 × 10^4 M^{-1} cm^{-1} for d(CGTTGC). Due to uncertainty in the molar extinction coefficient for the modified d(CGTTGC) strand, each DNA strand (about 1−2 mM) in D_2O was titrated into its complementary strand in the NMR tube while the intensity ratios of their characteristic base proton resonances were monitored at 60 °C. The samples were lyophilized and dissolved in 400 μL of 100 mM NaCl, 10 mM NaH_2PO_4, 2 mM NaN_3 buffer at pH 6 and then dried. For experiments in D_2O, the sample was lyophilized twice from 99.9% D_2O and finally redissolved in 400 μL of D_2O (99.96% enrichment). For experiments in H_2O, the sample was redissolved in 400 μL of 9:1 (v/v) H_2O-D_2O. All the chemical shifts in Table 2 are referenced to sodium 3-(trimethylsilyl)propionate-2,2,3,3-d_4 (TSP; δ = 0.00 ppm).

NMR Spectroscopy. All NMR spectra were recorded on a General Electric Ω500 spectrometer. One-dimensional spectra of exchangeable protons in H_2O were recorded using the spin−echo 1−1 pulse sequence with the carrier frequency at the solvent resonance to suppress the strong solvent peak.[44] The 1D NOE difference spectra were obtained by subtracting a reference spectrum irradiated off-resonance by the decoupler radio frequency (rf) from spectra irradiated at the desired peaks by the decoupler rf, collected into 8K data points by co-averaging 32 scans for each spectrum with 3000 total scans and a spectral width of 11 000 Hz.

Hypercomplex quadrature detection[45] was used to obtain pure-phase absorption mode DQF−COSY[46] and NOESY[47] spectra. The NOESY spectra were collected with mixing times of 50 and 200 ms at 1 °C for the backbone-modified DNA duplex and at 20 °C for its native counterpart. Phase-sensitive TOCSY spectra were recorded with use of the Waltz-16 spin-lock pulse to drive the coherence transfer, and a filter was inserted to remove the unwanted coherence transfer pathway by a novel phase cycling procedure which makes recording of the TOCSY spectra fairly routine.[48] Typical 2D data were collected with 512 FIDs with 2K data points each, 32−96 scans for each FID, a spectral width of 5600−6000 Hz, a 1-s predelay time in D_2O, and 1−1.5 s for solvent suppression. TOCSY spectra were collected with spin-lock times of 65, 80, and 100 ms to achieve direct, single, and multiple relayed through-bond magnetization transfer. Solvent was suppressed by continuous irradiation or selective excitation with the carrier set at the solvent resonance for spectra collected in H_2O. The data were apodized with a Lorentzian−Gaussian or phase-shifted sine-bell function. The first data point in t_1 was multiplied by 0.5 to suppress t_1 ridges[49] and also zero-filled in t_1 or symmetrized as necessary.

Structure Refinement. The distance constraints were derived from integration of the NOESY cross-peaks at mixing times of 50 and 200 ms. The integrals of cross-peak intensities were obtained and converted into distance constraints by the two-spin approximation for NOESY spectra collected at a mixing time of 200 ms due to the optimum signal-to-noise ratio of the spectrum for the volume integration. The possibility of spin diffusion artifacts was checked by control calculations, comparing ratios of cross-peak intensities of H6−H5, H6−CH_3, and H2′−H2″ to those of their corresponding distances by the two-spin approximation. Relative errors of 10% in distance were used as the estimates for both the upper and lower distance bounds.[19] However, particular care was taken to ensure that the NOE cross-peaks of the methylene protons on the modified linkage with the 5′-flanking sugar protons (Figure 6) were also present at the short, 50-ms mixing time by minimizing spin-diffusion artifacts for distance constraints (Supporting Information).

The initial structures were built and modified from standard B-DNA using the Biopolymer and Builder modules in InsightII. Energy

(42) Idziak, I.; Just, G.; Damha, M. J.; Giannaris, P. A. *Tetrahedron Lett.* **1993**, *34*, 5417.

(43) Pirrung, M. C.; Shuey, S. W.; Lever, D. C.; Fallon, L. *Bioorg Med. Chem. Lett.* **1994**, *4*, 1345.

(44) Sklenar, V.; Bax, A. *J. Magn. Reson.* **1987**, *74*, 469.

(45) States, D. J.; Haberkorn R. A.; Ruben D. J. *J. Magn. Reson.* **1982**,*48*, 286.

(46) Rance, M.; Sørensen, O. W.; Bodenhausen, G.; Wagner, G.; Ernst, R. R.; Wüthrich, K. *Biochem. Biophys. Res. Commun.* **1983**, *117*, 479.

(47) Macura, S.; Ernst, R. R. *Mol. Phys.* **1980**, *41*, 95.

(48) (a) Bax, A.; Davis, D. G. *J. Magn. Reson.* **1985**, *65*, 355. (b) Rance, M. *J. Magn. Reson.* **1987**, *74*, 557. (c) Luo, P.; Demetrios, T. B.; Subramanian, R. M.; Meredith, S. C.; Lynn, D. G. *Biochemistry* **1994**, *33*, 12367.

(49) Otting, G. H.; Widmer, G.; Wagner, G.; Wüthrich, K. *J. Magn. Reson.* **1986**, *66*, 187.

minimization and dynamic simulations were carried out using the Discover module in InsightII with the CVFF force field parameters. The hydrogen bonds in the Watson−Crick base pairs were constrained as supported by imino proton experiments to prevent dissociation of the two strands during simulations. The target functions for dynamic simulated annealing calculations are consisted of quadratic harmonic terms for covalent geometry, square well quadratic potentials for the NOE distance constraints and torsion angle constraints, and a quadratic van der Waals repulsion term for the nonbonded contacts.[50] The final structures was minimized by switching back to standard potential functions of the CVFF force field.

Thermal Melting and Data Analysis. Temperature-dependent ultraviolet spectra were measured with stirring on a Hewlett-Packard 8542A diode array spectrophotometer equipped with an HP89090A Peltier temperature controller. Data were analyzed using Kaleidagraph (Abelbeck Software). All data points were equally weighted unless otherwise stated, and errors reported for the fitted parameters are at the 67% confidence level.

Acknowledgment. We gratefully acknowledge the expertise of Paul Gardner in solid-phase DNA synthesis and thank Dr. Dean Astumian for the use of computing facilities and NIH, Biotechnology Training Grant (GM-08369) to J.C.L. and NIH Grant R21 RR12723 to D.G.L., for support.

Supporting Information Available: General synthetic procedures, the NOESY spectrum of the native DNA duplex, and the NOESY spectrum of the modified duplex showing the characteristic C7′−T3-H1′ cross-peak recorded with a 50-ms mixing time (7 pages). See any current masthead page for ordering information and Web access instructions.

JA972869W

(50) Nilges, M.; Clore, G. M.; Gronenborn, A. M. *FEBS Lett*. **1988**, *239*, 129.